REGULAR ARTICLE

Polymer Journal

Characterization of Linear Poly(*N*-isopropylacrylamide) and Cloud Points in its Aqueous Solutions

By Kunihiko KOBAYASHI, Satoshi YAMADA, Kouta NAGAOKA, Tomoaki KAWAGUCHI, Masashi OSA, and Takenao YOSHIZAKI*

The second virial coefficient A_2 and intrinsic viscosity $[\eta]$ were determined in methanol at 25.0 °C for poly(*N*-isopropylacrylamide) (PNIPA) samples synthesized by living anionic polymerization in the range of weight-average molecular weight M_w from 4.91×10^3 to 7.23×10^4, which are called L samples, and also for those by radical polymerization in *tert*-butanol and benzene by the use of azobis(isobutyronitrile) as an initiator in the range of M_w from 1.23×10^4 to 7.83×10^4, which are called T and B samples, respectively. It is found for both A_2 and $[\eta]$ that their values for the three kinds of samples agree well with each other in the range of $M_w \lesssim 3 \times 10^4$ but deviate from each other as M_w is increased from 3×10^4, the value for the L sample being the largest and that for the B sample the smallest. The result is consistent with the fact that the average chain dimension is the largest for the L sample having no branch point and the smallest for the B sample having the largest number of branch points. From a simultaneous analysis of A_2 and $[\eta]$ for the L samples on the basis of the Kratky–Porod wormlike chain with excluded volume, the stiffness parameter λ^{-1} is estimated to be 18 Å, which is almost the same as those determined for typical flexible polymers. For the L samples, the cloud point was also determined in their aqueous solutions in the range of the weight fraction w of PNIPA from *ca.* 0.5 to *ca.* 10%. It is found that the cloud point in the range of $w \gtrsim 2\%$ decreases from *ca.* 32 °C to *ca.* 18 °C as M_w is decreased from 7.23×10^4 to 5.47×10^3. Such behavior may be regarded as arising from effects of hydrophobic chain end groups of the L samples.

KEY WORDS: Poly(*N*-isopropylacrylamide) / Second Virial Coefficient / Intrinsic Viscosity / Wormlike Chain Model / Excluded-Volume Effect / Aqueous Solution / Cloud Point /

Recently, we have made a study of "phase" behavior of aqueous poly(*N*-isopropylacrylamide) (PNIPA) solutions,[1] which we had conventionally considered to be a well-defined model solution of a polar polymer in a polar solvent and to show lower-critical-solution-temperature (LCST) miscibility behavior.[2] Contrary to our optimistic expectation, however, the cloud points determined for aqueous solutions of PNIPA samples synthesized by radical polymerization in *tert*-butanol and methanol by the use of azobis(isobutyronitrile) (AIBN) as an initiator have been found to be definitely higher than those of samples synthesized in benzene and 1,4-dioxane, although the four kinds of samples had almost the same weight-average molecular weight M_w and stereochemical composition specified by the fraction f_r of racemo diads. In order to investigate the causes of such difference in the cloud point, we have examined the average chain dimensions of the PNIPA samples synthesized in *tert*-butanol and benzene, in dilute methanol (good solvent) solution.[3] The mean-square radius of gyration $\langle S^2 \rangle$, second virial coefficient A_2, and intrinsic viscosity $[\eta]$ have then been found to be larger for the former sample than for the latter, both having the same M_w and f_r. It has been concluded that the PNIPA samples synthesized by radical polymerization have branch points and the number of them is smaller in the sample synthesized in *tert*-butanol (or methanol) than in the one synthesized in benzene (or 1,4-dioxane). As a necessary continuation of the previous studies,[1,3] we make a further study of the cloud point of the aqueous solutions of well-characterized linear PNIPA samples properly synthesized, *e.g.*, living anionic polymerization, in order to investigate the effect of the branch points on the cloud point.

Preparation of linear PNIPA by living anionic polymerization requires a comment. It is known that anionic polymerization of *N*-isopropylacrylamide (NIPA) is unfeasible because of acidity of its amide proton.[4,5] Recently, however, it has been shown that linear PNIPA may be synthesized by anionic polymerization of "protected" NIPA whose amide proton is masked with a group properly chosen.[4–7] In this study, we adopt the Ishizone–Ito procedure by the use of NIPA masked with a methoxymethyl group along with diphenylmethylpotassium as an initiator,[5–7] which leads to a linear PNIPA sample having the same value of f_r ($\simeq 0.50$) as that of the previous samples synthesized by the radical polymerization ($f_r \simeq 0.52$).[1,3]

For the linear PNIPA samples so prepared, we first determine A_2 and $[\eta]$ in methanol (good solvent) and analyze them on the basis of the Kratky–Porod (KP) wormlike chain model.[8,9] We then determine the cloud points in aqueous solutions of the samples and compare the results so obtained with the previous ones for the PNIPA samples synthesized by radical polymerization.

Department of Polymer Chemistry, Kyoto University, Katsura, Kyoto 615-8510, Japan
*To whom correspondence should be addressed (E-mail: omasa@molsci.polym.kyoto-u.ac.jp).

 doi:10.1295/polymj.PJ2008315

EXPERIMENTAL

Materials

Following the Ishizone–Ito procedure,[5–7] linear PNIPA samples were prepared by hydrolysis of methoxymethyl groups of poly(*N*-methoxymethyl-*N*-isopropylacrylamide) [poly-(NMM-NIPA)] by the use of aqueous hydrochloric acid in 1,4-dioxane at room temperature for 10 h, where poly(NMM-NIPA) had been synthesized by living anionic polymerization of NMM-NIPA in tetrahydrofuran (THF) at −78 °C under high vacuum conditions for 24 h by the use of diphenylmethylpotassium as an initiator in the presence of diethyl zinc. The monomer NMM-NIPA was synthesized by the reaction of NIPA with chloromethylmethyl ether in the presence of potassium *tert*-butoxide in dry diethyl ether under dry nitrogen at 0 °C, where NIPA had been recrystallized three times from a 9/1 mixture of *n*-hexane and benzene and then dried in a vacuum for 12 h. The initiator diphenylmethylpotassium was synthesized by the reaction of diphenylmethane with potassium naphthalenide in dry THF under argon at room temperature, where potassium naphthalenide had been synthesized by the reaction of naphthalene with potassium. The polymerization of NMM-NIPA was terminated by adding methanol, so that the initiating and terminating chain ends of PNIPA are a diphenylmethyl group and a hydrogen atom, respectively.

Seven original samples so prepared were purified by reprecipitation from acetone solutions into *n*-hexane and then dialyzed seven times against pure water for 24 h by the use of a cellulose tube. By fractional precipitation using acetone as a solvent and *n*-hexane as a precipitant, each of the samples was separated into three fractions, the middle of them being used as a test sample. The seven test samples were freeze-dried from their 1,4-dioxane solutions after filtration through a Teflon membrane of pore size 1.0 μm.

Besides the above linear PNIPA samples, we also synthesized two PNIPA samples by radical polymerization with AIBN as an initiator, in the same manner as in the previous study.[1] One sample was synthesized in *tert*-butanol and the other in benzene. We note that chain ends of the PNIPA samples are considered to be isobutyronitrile groups derived from AIBN, although detailed information could not be obtained. The samples so synthesized were purified and then separated into several fractions of narrow molecular-weight distribution, in the above-mentioned manners. Three and two fractions from the samples synthesized in *tert*-butanol and benzene, respectively, were used as test samples and were freeze-dried in the above-mentioned manner.

In the first column of Table I are given the codes of all the samples synthesized in this work. We use the letter L for the samples synthesized by living anionic polymerization and the letters T and B for those synthesized by radical polymerization in *tert*-butanol and benzene, respectively, and call the samples generally as L, T, and B samples, for convenience. In the second column of the table are also given the values of the ratio M_w/M_n of M_w to the number-average molecular weight M_n, which were determined from analytical gel permeation chromatography (GPC) in the same manner as before[1] using THF as an eluent and 12 standard polystyrene samples (Tosoh, $M_w = 2.8 \times 10^3$–8.4×10^6, $M_w/M_n = 1.02$–1.17) as reference standards.

Table I. Values of M_w/M_n and f_r and results of LS and viscosity measurements for poly(*N*-isopropylacrylamide) in methanol at 25.0 °C

sample	M_w/M_n[a]	f_r	M_w	$10^4 A_2$ (cm^3 mol/g^2)	$[\eta]$ (dL/g)	k'
samples synthesized by living anionic polymerization						
L0.5	1.23	0.51	4.91×10^3	11.8	0.076_3	0.59
L0.6	1.12	0.49	5.47×10^3	11.5	0.080_6	0.59
L1	1.16	0.50	8.98×10^3	9.1_2	0.103	0.53
L2	1.12	0.51	2.21×10^4	7.1_5	0.175	0.47
L3	1.08	0.51	3.11×10^4	6.9_6	0.235	0.46
L6	1.09	0.51	5.64×10^4	5.8_4	0.367	0.39
L7	1.12	0.50	7.23×10^4	5.6_4	0.413	0.41
samples synthesized by radical polymerization in *tert*-butanol						
T1	1.29	0.52	1.23×10^4	8.5_5	0.125	0.54
T3	1.25	0.52	2.76×10^4	6.6_5	0.204	0.57
T4	1.29	0.52	4.23×10^4	6.1_1	0.280	0.42
samples synthesized by radical polymerization in benzene						
B3	1.26	0.52	2.90×10^4	6.5_9	0.206	0.43
B8	1.28	0.52	7.83×10^4	4.7_3	0.398	0.39

[a]The values of M_w/M_n were determined by analytical GPC using standard PS samples as reference standards.

The solvent methanol used for static light scattering and viscosity measurements was purified by distillation after refluxing over calcium hydride for *ca.* 6 h. The solvent THF used for analytical GPC was of reagent grade with no stabilizer. The solvent deuterated dimethyl sulfoxide (DMSO) used for ^{1}H NMR spectroscopy was of reagent grade. The solvent water used for the determinations of the cloud point was highly purified through a Simpli Lab water purification system of Millipore Co., its resistivity being 18.2 MΩ·cm.

^{1}H NMR

^{1}H NMR spectra for all the samples in deuterated DMSO at 170 °C were recorded on a JEOL EX-400 spectrometer at 399.8 MHz by the use of an rf pulse angle of 90° with a pulse repetition time of 8 s, where tetramethylsilane was added to each test solution as an internal standard.

Light Scattering

Light scattering (LS) measurements were carried out to determine M_w and the second virial coefficient A_2 for all the samples in methanol at 25.0 °C. A Fica 50 light-scattering photometer was used for all the measurements with vertically (v) polarized incident light of wavelength $\lambda_0 = 436$ nm. For a calibration of the apparatus, the intensity of light scattered from pure benzene was measured at 25.0 °C at a scattering angle of 90°, where the Rayleigh ratio $R_{Uu}(90°)$ of pure benzene was taken as 46.5×10^{-6} cm^{-1}.[10] The depolarization ratio ρ_u of pure benzene at 25.0 °C was determined to be 0.41 ± 0.01. Scattered intensity was measured at seven or eight different concentrations and at scattering angles θ ranging from 30.0 to 142.5°, and then converted to the excess unpolarized (Uv)

components ΔR_{Uv} of the reduced scattered intensity by the use of the scattered intensity from the solvent methanol. The data obtained were treated by using the Berry square-root plot.[11] It was found that the corrections for the optical anisotropy were necessary to estimate true M_w and A_2 for samples with $M_w \lesssim 8 \times 10^3$, and therefore the excess depolarized (HV) components ΔR_{Hv} of the reduced scattered intensity necessary for the corrections were also measured for them. As for samples with $M_w \gtrsim 8 \times 10^3$, the corrections were unnecessary since effects of optical anisotropy were very small.

The most concentrated solution of each sample was prepared gravimetrically and made homogeneous by continuous stirring at room temperature for 1–3 d. It was optically purified by filtration through a Teflon membrane of pore size 0.10 μm. The solutions of lower concentrations were obtained by successive dilution. The weight concentrations of the test solutions were converted to the polymer mass concentrations c by the use of the densities of the respective solutions calculated with the partial specific volumes v_2 of the samples and with the density of the solvent methanol. The quantity v_2 was measured by using an oscillating U-tube density meter (Anton-Paar, DMA5000). The values of v_2 so determined in methanol at 25.0 °C are 0.893, 0.892, 0.904, 0.901, 0.901, 0.901, 0.901, 0.901, 0.902, 0.902, 0.892, and 0.903 cm^3/g for the samples L0.5, L0.6, L1, L2, L3, L6, L7, T1, T3, T4, B3, and B8, respectively. For the value of ρ_0 of methanol at 25.0 °C, we used the literature value 0.7866 g/cm^3.[12]

The refractive index increment $\partial n/\partial c$ was measured at the wavelength of 436 nm by the use of a Shimadzu differential refractometer DR-1. The values of $\partial n/\partial c$ in methanol at 25.0 °C were determined to be 0.188_9, 0.186_7, 0.187_6, 0.183_9, 0.184_1, 0.184_2, 0.184_3, 0.184_2, 0.183_6, 0.183_8, 0.184_1, and 0.184_9 cm^3/g for the samples L0.5, L0.6, L1, L2, L3, L6, L7, T1, T3, T4, B3, and B8, respectively. For the refractive index n_0 of methanol at 25.0 °C at the wavelength of 436 nm, we used the literature value 1.3337.[12]

Viscosity

Viscosity measurements were carried out for all the samples in methanol at 25.0 °C by the use of conventional capillary and four-bulb spiral capillary viscometers of the Ubbelohde type. The flow time was measured to a precision of 0.1 s, keeping the difference between those of the solvent and solution larger than 20 s. The test solutions were maintained at a constant temperature within ±0.005 °C during the measurements.

The most concentrated solution of each sample was prepared in the same manner as in the case of the LS measurements. The solutions of lower concentrations were obtained by successive dilution. The polymer mass concentrations c were calculated from the weight fractions with the densities of the solutions. Density corrections were also made in the calculations of the relative viscosity η_r from the flow times of the solution and solvent. The data obtained for the specific viscosity η_{sp} and η_r in the range of $\eta_r < 1.4$ were treated as usual by the Huggins (η_{sp}/c *vs.* c) and Fuoss–Mead ($\ln \eta_r/c$ *vs.* c) plots, respectively, to determine $[\eta]$ and the Huggins coefficient k'. (Note that the two plots have the same intercept.)

Transmittance of Light

The intensity of light passing through the aqueous solution of the five L samples at a given weight fraction w of the sample was monitored. All the measurements were carried out by the use of a self-made apparatus with incident light of wavelength 650 nm from a laser diode module, as described below. A cylindrical cell of outer diameter 10 mm containing a given test solution was immersed in a water bath, the test solution in the cell being stirred continuously.

In order to determine the cloud point of each solution, the temperature of the water bath was controlled to increase at the rate of *ca.* 1.5 °C/h. During continuous increase in temperature from 15 °C to 30 °C for the sample L0.6, from 17 °C to 32 °C for the sample L1, from 18 °C to 32 °C for the sample L2, from 20 °C to 33 °C for the sample L3, and from 26 °C to 34 °C for the sample L7, the intensity of light passing through the cell was monitored by a photodiode. The output of the photodiode along with the solution temperature measured simultaneously by the use of a platinum resistance thermometer combined with a programmable digital multimeter (Yokokawa 7555) was recorded on a personal computer at intervals of 10 s. Then, the (relative) transmittance as defined as the ratio of the intensity of light through a test solution at a temperature to that at a lower temperature at which the test solution may be regarded as transparent was determined as a function of temperature. The measurements were carried out at 8 different concentrations in the range of $0.5 \lesssim w \lesssim 10\%$ for each sample. The most concentrated solution of each sample was prepared gravimetrically and made homogeneous by continuous stirring for 2 d at *ca.* 5 °C. The solutions of lower concentrations were obtained by successive dilution at *ca.* 5 °C.

RESULTS

Stereochemical Composition

Figure 1 shows ^{1}H NMR spectra for the samples L0.5 and L7 (synthesized by living anionic polymerization) over the whole range of the chemical shift δ (in units of ppm) in which all the signals from PNIPA, *i.e.*, the methylene (a) and methine (b) protons in the main chain and the amide (c), methine (d), and methyl (e) protons in the side group, are included. According to Isobe *et al.*,[13] the three signals from the a protons in the range of $1.2 \lesssim \delta \lesssim 1.8$ may be assigned to those in the meso (m), racemo (r), and m diads, respectively, from the right to the left, as shown in the spectrum for L0.5. At $\delta \simeq 7.2$, the signals from the phenyl groups at the initiating end may be definitely observed (∗) for L0.5, while those for L7 are very weak.

In the third column of Table I are given the values of f_r determined from the relative intensities of the three signals from the a protons. It is seen from the values of f_r that all the PNIPA samples synthesized in this work have almost the same stereochemical composition irrespective of the polymerization method, *i.e.*, living anionic or radical polymerization.

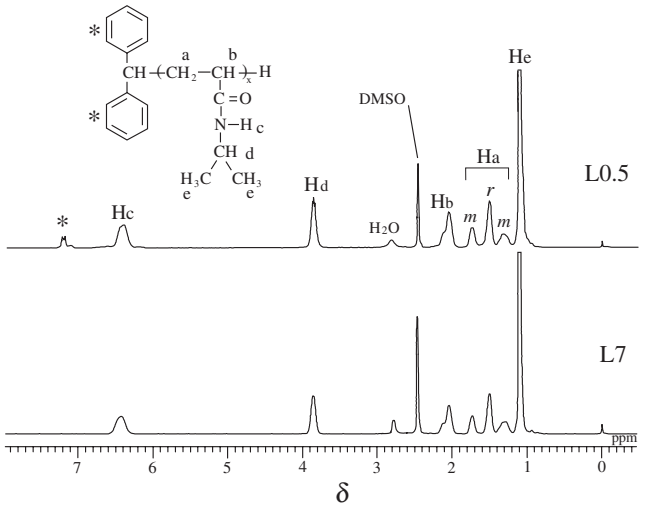

Figure 1. ^{1}H NMR spectra for the PNIPA samples L0.5 and L7. The signal indicated by the asterisk may be assigned to the phenyl protons at the initiating end of the PNIPA samples.

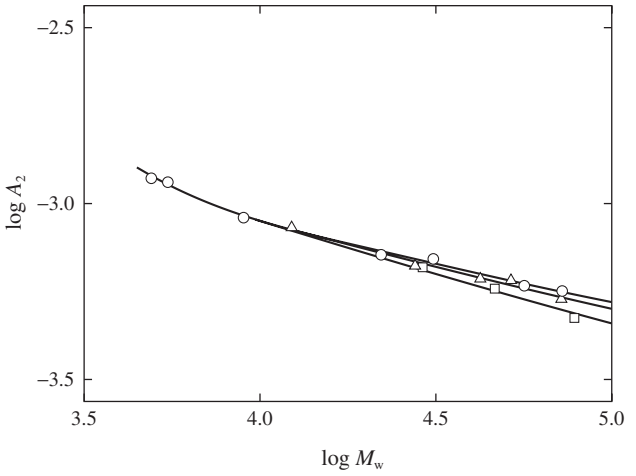

Figure 2. Double-logarithmic plots of A_2 (in cm^3 mol/g^2) against M_w for PNIPA in methanol at 25.0 °C: (○) L samples; (△) T samples; (□) B samples. The solid curve connects smoothly the data points for the respective samples.

Second Virial Coefficient in Methanol at 25 °C

The values of M_w and A_2 determined from LS measurements in methanol at 25.0 °C are given in the fourth and fifth columns, respectively, of Table I, where the corrections for the optical anisotropy to M_w and A_2 were made for the samples L0.5 and L0.6 following the standard procedure,[14–18] as done in previous studies.[19,20] We omit here the details of the corrections and only note that the values of the optical anisotropy factor δ determined from ΔR_{Uv} and ΔR_{Hv} are $9.9_3 \times 10^{-3}$ and $6.7_5 \times 10^{-3}$ for L0.5 and L0.6, respectively. From the relative intensities of the ^{1}H NMR signals from the phenyl groups at the initiating end of the L samples (see Figure 1), we have been able to estimate M_n of L0.5 and L0.6 to be 4.2×10^3 and 4.7×10^3, respectively, which are rather in good agreement with the M_n values 4.0×10^3 and 4.9×10^3 estimated for L0.5 and L0.6, respectively, from the values of M_w and M_w/M_n given in Table I. For the other L samples, the intensities of the ^{1}H NMR signals from the terminal group are not strong enough to estimate M_n accurately. The values of A_2 are of order 10^{-3}–10^{-4} cm^3 mol/g^2 for all the samples, indicating that methanol at 25.0 °C is a good solvent for them irrespective of the polymerization method.

Figure 2 shows double-logarithmic plots of A_2 (in cm^3 mol/g^2) against M_w for PNIPA in methanol at 25.0 °C. The circles, triangles, and squares represent the values for the L, T, and B samples, respectively, and the solid curve connects smoothly the data points for the respective samples. We note that there are also plotted the data points for the samples T5 ($M_w = 5.17 \times 10^4$), T7 (7.19×10^4), and B5 (4.65×10^4) which have been reproduced from Figure 2 of ref 3 (see also Table II of ref 3). It is seen that the data points for the three kinds of samples agree well with each other in the range of small M_w ($\lesssim 3 \times 10^4$) and the data points for the T and B samples deviate downward progressively from those for the L samples with increasing M_w ($\gtrsim 3 \times 10^4$), the value of A_2 for the B sample being the smallest at a given M_w.

It has been shown in the previous paper[3] that the PNIPA samples synthesized by radical polymerization have a small number of branch points, which is larger for the B sample than for the T one at a given M_w. The quantity A_2 is proportional to an effective volume excluded to one polymer chain by the presence of another, and it may be considered to decrease with increasing the number of branch points. The above result that A_2 for the L sample having no branch point is the largest of all at a given M_w is therefore consistent with the previous conclusion.[3]

As is well known, effects of chain ends on A_2 become remarkably large in the range of small M_w, including oligomers.[9,21–26] The slope of the plots in the range of $M_w \lesssim 10^4$, where the A_2 values for the L, T, and B samples agree with each other, is *ca.* −0.34 and is appreciably steeper than the asymptotic value −0.2 for linear flexible polymers with very large M_w. This is due to the effects of chain ends. The agreement between the A_2 values in the range of small M_w implies that the number of the branch points in the T and B samples is negligibly small if any and the difference in the end group does not appreciably affect A_2 in methanol at 25.0 °C.

Intrinsic Viscosity in Methanol at 25 °C

The values of $[\eta]$ and k' determined from viscosity measurements in methanol at 25.0 °C are given in the sixth and seventh columns, respectively, of Table I. Figure 3 shows double-logarithmic plots of $[\eta]$ (in dL/g) against M_w for PNIPA in methanol at 25.0 °C. The symbols and curves have the same meaning as those in Figure 2. We note that there are also plotted the data points for the samples T5, T7, and B5 which have been reproduced from Figure 3 of ref 3 (see also Table II of ref 3). As in the case of A_2 shown in Figure 2, the data points for the three kinds of samples agree well with each other in the range of small M_w ($\lesssim 3 \times 10^4$) and the data points for the T and B samples deviate downward progressively from those for the L samples with increasing M_w ($\gtrsim 3 \times 10^4$), the

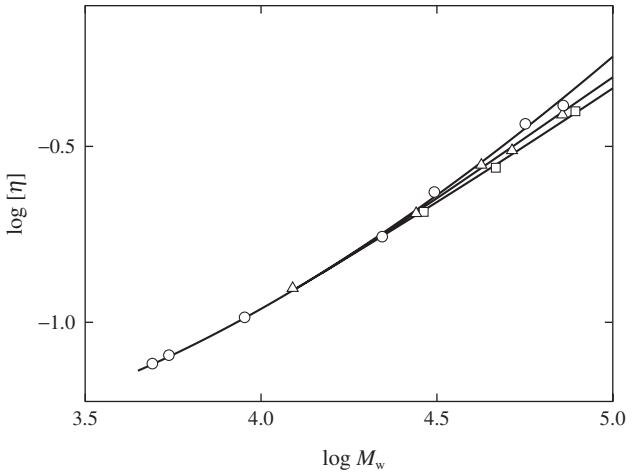

Figure 3. Double-logarithmic plots of [η] (in dL/g) against M_w for PNIPA in methanol at 25.0 °C. The symbols and curves have the same meaning as those in Figure 2.

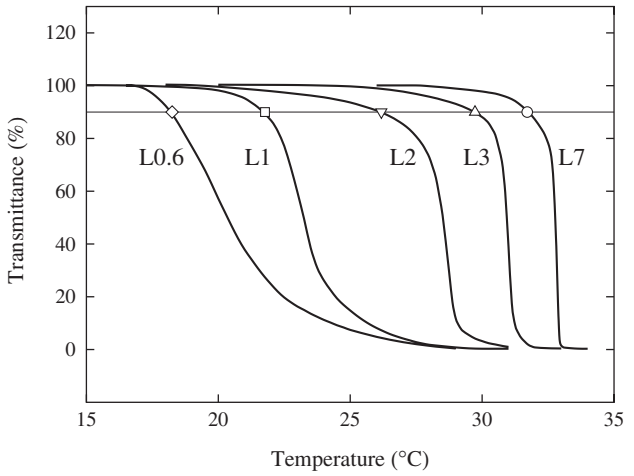

Figure 4. Temperature dependence of the transmittance of light passing through aqueous solutions of the PNIPA samples L0.6, L1, L2, L3, and L7 at $w = 5.03$, 4.97, 4.94, 4.93, and 4.94%, respectively, the symbols ◇, □, ▽, △, and ○ representing the respective cloud points (see the text).

value of [η] for the B sample being the smallest at a given M_w. Since [η] proportional to the hydrodynamic volume is considered to decrease with increasing the number of branch points, the above result for [η] is consistent with that for A_2 in the previous subsection. The agreement between the [η] values in the range of small M_w indicates that the number of the branch points in the T and B samples is negligibly small if any. The slope of the plot for each sample increases with increasing M_w because of the intramolecular excluded-volume effect.

Cloud Point in Aqueous Solutions

Figure 4 shows plots of the (relative) transmittance of light through the aqueous solutions of the PNIPA samples L0.6, L1, L2, L3, and L7 at the weight fraction $w = 5.03$, 4.97, 4.94, 4.93, and 4.94%, respectively, against temperature. Here, the (relative) transmittance is defined as the ratio of the intensity of light passing through a test solution at a temperature to that at a lower temperature at which the test solution may be regarded as transparent. We note that the shape of the transmittance curve for each solution is almost independent of the rate of increase in temperature if it is slower than 1.5 °C/h. It is seen that the transmittance curve shifts toward the low-temperature side and the decrease in the transmittance becomes gentle, with decreasing M_w.

The cloud point is experimentally determined to be the temperature at which a given test solution just begins to be turbid, *i.e.*, its transmittance just starts to decrease from 100%, in the heating process. As seen from Figure 4, it is difficult to determine such a temperature unambiguously, so that we adopt the temperature at which the transmittance becomes 90% as the cloud point, for convenience, following the previous study.[1] The symbols ◇, □, ▽, △, and ○ in Figure 4 represent the cloud points so determined for the samples L0.6, L1, L2, L3, and L7, respectively. The cloud points for the aqueous solutions of the samples L0.6, L1, L2, L3, and L7 at other w's have also been determined in the same manner as mentioned above.

DISCUSSION

Chain Stiffness in Methanol at 25 °C

As far as we know, there has not yet been made polymer molecular characterization of PNIPA on the basis of its dilute solution properties, and therefore there is no available information about its chain stiffness. Since the PNIPA samples used so far in studies of their solutions are synthesized by radical polymerization and consequently have branched structures,[3] the stiffness of the PNIPA chain could not be correctly estimated from their solution properties. Fortunately, however, we were able to prepare the series of linear PNIPA samples, *i.e.*, L samples, by living anionic polymerization, and analyze the data for their A_2 and [η] in order to estimate the stiffness.

As shown in previous studies of dilute solution properties of various vinyl polymer chains, they prefer to take locally curved or helical conformations, so that the helical wormlike (HW) chain is suitable for the analysis of their solution properties.[9,27] It is therefore desirable to analyze the present data for the L samples on the basis of the HW chain. Unfortunately, however, the range 5×10^3–7×10^4 of M_w of the L samples is not sufficiently wide to determine unambiguously all the HW model parameters from a comparison of the HW theory with the experimental data. Then we adopt the KP chain[8,9] as the second best model.

Before proceeding to make a comparison of theory with experiment, we briefly summarize the KP theory of A_2 and [η]. The KP chain is an elastic wire with bending energy immersed in a thermal bath, whose statistical behavior may be characterized by the stiffness parameter λ^{-1} having the dimension of length.[9] We note that the chain becomes stiff with increasing λ^{-1}, and the two limits of $\lambda^{-1} \to 0$ and ∞ correspond to the random coil and rigid rod, respectively. We also note that the HW chain is also an elastic wire with torsional energy in

addition to the bending one and includes the KP chain as a special case. The total contour length L of the KP chain is related to the molecular weight M of a real polymer chain by

$$L = M/M_L \tag{1}$$

where M_L is the shift factor as defined as the molecular weight per unit contour length of the KP chain. The equilibrium conformational behavior of the KP chain without excluded volume may then be described by the two parameter λ^{-1} and M_L.

According to the Yamakawa theory,[9,21] A_2 of the KP chain may be written in the form,

$$A_2 = A_2^{(HW)} + A_2^{(E)} \tag{2}$$

where $A_2^{(HW)}$ is a part of A_2 without effects of chain ends and $A_2^{(E)}$ represents a contribution of the effects. We note that the superscript (HW) has been attached since the theory is originally formulated on the basis of the HW chain. In the theory, the excluded volume is incorporated by $n+1$ beads arrayed with spacing a between them along the KP chain contour, so that $L = na$. The $n-1$ intermediate beads are identical and the two end beads are different from the intermediate ones and also from each other in species. Identical excluded-volume interactions between intermediate beads are expressed in terms of the binary cluster integral β, which characterizes $A_2^{(HW)}$. In addition to β, two kinds of excess binary-cluster integrals β_1 and β_2 are introduced to express interactions between unlike (and like end) beads, β_1 being associated with one end bead and β_2 with two end beads, which characterize $A_2^{(E)}$.

The first term $A_2^{(HW)}$ on the right-hand side of eq 2 may be written in the form,

$$A_2^{(HW)} = \frac{N_A B}{2{M_L}^2} h\left(\frac{\tilde{\tilde{z}}}{\alpha_S{}^3(\tilde{z})}\right) \tag{3}$$

where N_A is the Avogadro constant, B is the excluded-volume strength defined by

$$B = \beta/a^2 \tag{4}$$

and h is the so-called h function that is the dimensionless function of the *intermolecular* scaled excluded-volume parameter $\tilde{\tilde{z}}$ divided by the cube of the gyration-radius expansion factor α_S as a function of the *intramolecular* scaled excluded-volume parameter $\tilde{z}$. The dimensionless quantities $\tilde{z}$ and $\tilde{\tilde{z}}$ are related to the (conventional) excluded-volume parameter z defined by

$$z = (3/2\pi)^{3/2}(\lambda B)(\lambda L)^{1/2} \tag{5}$$

by

$$\tilde{z} = \frac{3K(\lambda L)}{4} z \tag{6}$$

and

$$\tilde{\tilde{z}} = \frac{Q(\lambda L)}{2.865} z \tag{7}$$

respectively, where K and Q as functions of the reduced contour length λL represent effects of the chain stiffness on the intra- and intermolecular excluded-volume effects, respectively. Both the factors $3K/4$ and $Q/2.865$ become unity in the limit of $\lambda L \to \infty$ (random coil), so that $\tilde{z} = \tilde{\tilde{z}} = z$ and the above expression for $A_2^{(HW)}$ reduces to that of A_2 in the framework of the (conventional) two-parameter (TP) theory.[9,14] In the limit of $\lambda L \to 0$ (rigid rod), on the other hand, K and therefore $\tilde{z}$ (intramolecular excluded volume) vanishes. The h function is given by eq 8.110 of ref 9 (or eq 14 of ref 20), the Domb–Barrett equation[28] given by eq 8.57 of ref 9 (or eq 6 of ref 20) is adopted for α_S, and K and Q are given by eqs 8.46 and 8.102 of ref 9 (or eqs 8 and 17 of ref 20), respectively. We do not reproduce their explicit forms, for simplicity.

The second term $A_2^{(E)}$ on the right-hand side of eq 2 may be written in the form,

$$A_2^{(E)} = \frac{2N_A\beta_1}{M_0}\frac{1}{M} + 2N_A(\beta_2 - 2\beta_1)\frac{1}{M^2} \tag{8}$$

with M_0 the molecular weight of the bead. We note that $A_2^{(E)}$ rapidly decreases to 0 with increasing M and has been shown to be very small for $M \gtrsim 10^5$ for all the vinyl polymers examined so far.[9,22–25] It is seen from eqs 1–7 that the theoretical values of A_2 may be calculated for a given polymer by the use of proper values of λ^{-1}, M_L, and λB along with β_1 and β_2.

As in the cases of other vinyl polymers, we adopt the touched-bead model as a hydrodynamic model,[9] in which N identical spherical beads of diameter d_b are arrayed with spacing d_b between them along the KP chain of total contour length $L = Nd_b$, its $[\eta]$ $(= [\eta]_0)$ without excluded volume may be written in the form,[9,29]

$$[\eta]_0 = \frac{1}{\lambda^2 M_L} f_{\eta,KP}(\lambda L; \lambda d_b) \tag{9}$$

where $f_{\eta,KP}$ as a function of λL and the reduced bead diameter λd_b is defined by

$$f_{\eta,KP}(\lambda L; \lambda d_b) = \lambda^{-1} M_L [\eta]_{KP} \tag{10}$$

with $[\eta]_{KP}$ being given by eq 6.111 with eqs 6.113 and 6.117 of ref 9 (or eq 15 with eqs 17 and 22 of ref 29). We note that $[\eta]_{KP}$ in refs 9 and 29 is written in units of $(\lambda^{-1})^3$ and the quantities L and d_b in those references means the reduced quantities λL and λd_b, respectively. We do not reproduce the explicit form of $[\eta]_{KP}$, for simplicity.

In the framework of the quasi-two-parameter (QTP) scheme or the Yamakawa–Stockmayer–Shimada scheme[9,30–32] on the basis of the HW (or KP) chain, $[\eta]$ of the KP touched-bead model with excluded volume may be given by

$$[\eta] = [\eta]_0 \alpha_\eta^3(\tilde{z}) \tag{11}$$

where $[\eta]_0$ is given by eq 9 and α_η is the viscosity-radius expansion factor as a function of $\tilde{z}$ and may be given by the Barrett equation,[33] whose explicit form is not reproduced here, for simplicity. We note that all the expansion factors, including α_η, are functions only of $\tilde{z}$, in the QTP scheme. Then the theoretical values of $[\eta]$ may be calculated for a given polymer by the use of proper values of λ^{-1}, M_L, λB, and λd_b.

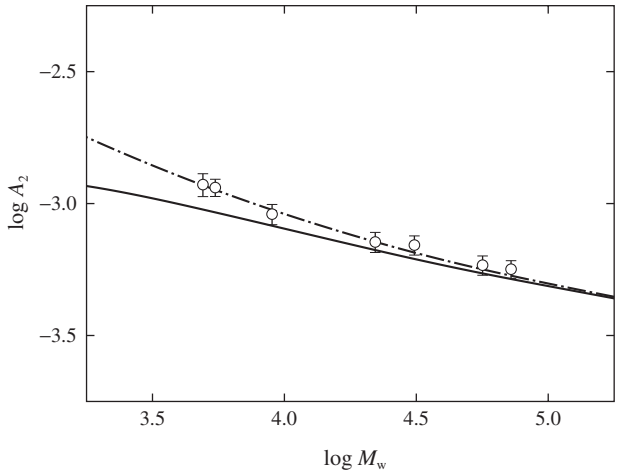

Figure 5. Double-logarithmic plots of A_2 (in $cm^3\ mol/g^2$) against M_w for the L samples in methanol at 25.0 °C. The solid curve represents the best-fit KP theory values without the effects of chain end and the dot-dashed curve represents those with the effects (see the text).

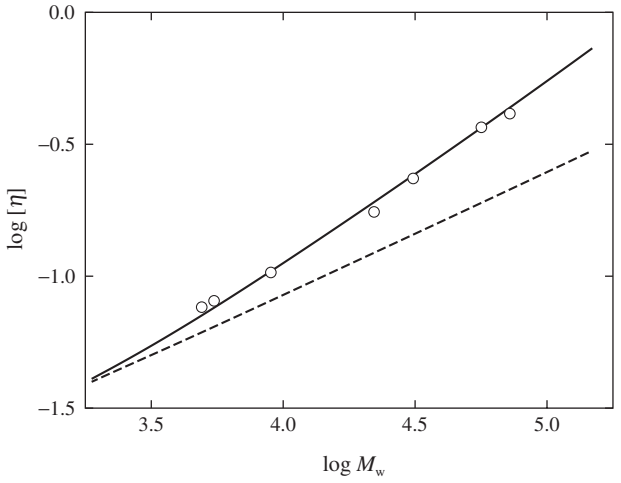

Figure 6. Double-logarithmic plots of [η] (in dL/g) against M_w for the L samples in methanol at 25.0 °C. The solid curve represents the best-fit perturbed KP theory values and the dashed curve represents the corresponding unperturbed values (see the text).

Now we are in a position to make a comparison of KP theories of A_2 and [η] with the experimental data, from which we may in principle determine the values of λ^{-1}, M_L, λB, and λd_b along with β_1 and β_2 for linear PNIPA. As mentioned above, however, the range of M_w of the linear PNIPA samples is not wide enough to determine unambiguously all those parameters. Further, the double-logarithmic plots of A_2 and [η] against M_w shown in Figures 2 and 3 (○), respectively, do not have any characteristic features but are rather monotonous over the whole range of M_w examined. In order to reduce the number of the parameters to be determined, therefore, we assume the value of M_L to be 45 $Å^{-1}$, which has been calculated from the value 113 of the molecular weight of the repeat unit and its length[34,35] 2.5 Å in the all-*trans* conformation. We then attempt to determine the three parameters λ^{-1}, λB, and λd_b from a simultaneous comparison of the KP theories of A_2 and [η] with the experimental data. For A_2, the comparison is restricted to the range of $M_w \gtrsim 5 \times 10^4$ where the effects of chain ends is considered to be sufficiently small to neglect the contribution of $A_2^{(E)}$ on the right-hand side of eq 2. As for the data for A_2 in the range of $M_w \lesssim 5 \times 10^4$, we analyze them to evaluate β_1 and β_2 included in $A_2^{(E)}$ given by eq 8 by the use of the values of $A_2^{(HW)}$ calculated from eq 3 with the values of λ^{-1} and λB so determined.

Figures 5 and 6 show double-logarithmic plots of A_2 (in $cm^3\ mol/g^2$) and [η] (in dL/g) against M_w for the L samples in methanol at 25.0 °C, where the solid curves represent the best-fit KP theory values of A_2 without the effects of chain ends, *i.e.*, $A_2^{(HW)}$, calculated from eq 3 with eqs 4–7 and those of [η] calculated from eq 11 with eqs 9 and 10, respectively, with $\lambda^{-1} = 18$ Å, $\lambda B = 0.60$, and $\lambda d_b = 0.58$. We note that relative errors in the values of λ^{-1}, λB, and λd_b are estimated to be ±10%, ±15%, and ±12%, respectively, at most. The value 18 Å of λ^{-1} so determined is almost the same as the values $\lambda^{-1} = 20.6$–27.0 Å and 12.7–18.7 Å determined for atactic polystyrene (a-PS) with $f_r = 0.59$ in cyclohexane at 34.5 °C (Θ) and polyisobutylene (PIB) in isoamyl isovalerate at 25.0 °C (Θ),[9] respectively, indicating that PNIPA in methanol is as flexible as typical flexible polymers. The value 10.4 Å of d_b evaluated from the above-mentioned values of λ^{-1} and λd_b seems reasonable.

In Figure 5, the experimental value deviates upward progressively from the $A_2^{(HW)}$ value (solid curve) as M_w is decreased from *ca.* 5×10^4 because of the effects of chain ends. The dot-dashed curve in the figure represents the value of A_2 calculated from eq 2 with the $A_2^{(HW)}$ value represented by the solid curve and the $A_2^{(E)}$ calculated from eq 8 with the values 100 and 210 $Å^3$ of β_1 and β_2, respectively, where we have taken the monomer unit of the PNIPA chain as a single bead ($M_0 = 113$). We note that the values of β_1 and β_2 for PNIPA in methanol at 25.0 °C are comparable to those obtained for other flexible polymers in good solvents.[22–25]

In Figure 6, the dashed curve represents the unperturbed value $[\eta]_0$ of [η] calculated from eq 9 with eq 10 with the above-mentioned values of λ^{-1} and λd_b. It is seen that the experimental value deviates upward progressively from the $[\eta]_0$ value as M_w is increased because of the intramolecular excluded-volume effect.

It should be noted here that the PNIPA chain in aqueous solution might become stiffer than that in methanol due to the hydration of the solvent water. Unfortunately, however, it is difficult to carry out fine molecular characterization of the chain in aqueous solution in the same manner as above, since the cloud point in aqueous PNIPA solution remarkably decreases with decreasing temperature, as shown in the previous subsection.

Cloud-Point Curve in Aqueous Solutions

Figure 7 shows cloud-point curves in aqueous PNIPA solutions. The unfilled symbols represent the cloud points for

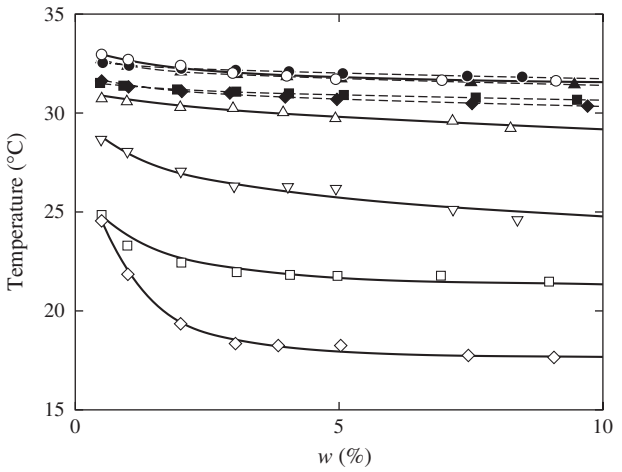

Figure 7. Cloud-point curves in aqueous PNIPA solutions. The unfilled symbols represent the cloud points in aqueous solutions of the L samples L0.6 (◇), L1 (□), L2 (▽), L3 (△), and L7 (○) and the filled symbols represent those of the T and B samples T5 (▲), T13 (●), B5 (◆), and B14 (■) which have been reproduced from Figure 3 of ref 1. The solid and dashed curves connect smoothly the cloud points of the L samples and the T and B samples, respectively.

the L samples L0.6 (◇), L1 (□), L2 (▽), L3 (△), and L7 (○), and the filled symbols represent those previously determined for the T and B samples T5 (▲) with $M_w = 5.17 \times 10^4$, T13 (●) with $M_w = 1.31 \times 10^5$, B5 (◆) with $M_w = 4.65 \times 10^4$, and B14 (■) with $M_w = 1.44 \times 10^5$, which have been reproduced from Figure 3 of ref 1. The solid and dashed curves connect smoothly the cloud points for the L samples and the T and B samples, respectively. We note that all the L, T, and B samples have almost the same values of f_r (= 0.50–0.52).

It is interesting to see that the cloud point in the aqueous solutions of the L samples decreases remarkably with decreasing M_w, especially in the range of rather large w ($\gtrsim 2\%$). Such behavior sharply contradicts the familiar conclusion derived from the polymer solution thermodynamics. It is known that amphiphilic A-B diblock[36,37] or A-B-A triblock[38] copolymers with the B block being PNIPA form aggregates and the cloud points in their aqueous solutions are lower than that in aqueous PNIPA solution. Further, it was pointed out by Ito and Ishizone[7] that the hydrophobic diphenylmethyl group at the initiating end of the L sample affects the cloud points in its aqueous solutions. For PNIPA samples synthesized by radical polymerization, it was also pointed out by Duan *et al.*[39] and by Furyk *et al.*[40] that the cloud points of their aqueous solutions become lower as hydrophobicity of the end group is increased. It may therefore be considered that the cloud point in aqueous solutions of the L samples is mainly governed by the diphenylmethyl group and decreases as its effect is relatively increased by decreasing M_w.

At first we expected that the cloud points in the aqueous solutions of the L samples without branch points would be higher than those for the T and B samples with branch points, since the cloud point decreases with increasing the number of branch points.[1,3] As seen from Figure 7, however, the cloud point in the range of $w \gtrsim 3\%$ is still lower for L7 than for T13 due to the effect of the diphenylmethyl group whose hydrophobicity seems to be larger than that of the isobutyronitrile group at the ends of the T and B samples. In this connection, we may conjecture that the decrease in the cloud point with decreasing M_w and with increasing the number of branch points observed previously[1,3] (and also shown by the filled symbols in Figure 7) for the aqueous solutions of the T and B samples is also caused by the hydrophobicity of the end group.

Considering the above-mentioned situation along with the fact that the transmittance curves shown in Figure 4 do not show sharp decrease as usually observed in common LCST miscibility behavior, there arises a doubt that the cloud point determined from the transmittance of the light through the aqueous PNIPA solutions does not necessarily correspond to the binodal point, at which the macroscopic phase separation occurs.

CONCLUDING REMARKS

We have determined A_2 and $[\eta]$ in methanol at 25.0 °C for the PNIPA samples synthesized by living anionic polymerization following the procedure of Ishizone and Ito,[5–7] which we call L samples, and also for those by radical polymerization in *tert*-butanol and benzene by the use of AIBN as an initiator, which we call T and B samples, respectively. Note that the L samples are linear while the T and B samples have a small number of branch points. It has been found for both A_2 and $[\eta]$ that their values for the three kinds of samples agree well with each other in the range of small M_w ($\lesssim 3 \times 10^4$) but deviate from each other as M_w is increased from 3×10^4, the value for the L sample being the largest and that for B sample the smallest. Such deviations may be regarded as arising from the difference in the primary structure of the samples, *i.e.*, the average chain dimension is the largest for the L sample having no branch point and the smallest for the B sample having the largest number of branch points. The number of the branch points in the T and B samples seems to become very small for $M_w \lesssim 3 \times 10^4$. From a simultaneous analysis of A_2 and $[\eta]$ for the L samples on the basis of the KP chain with excluded volume, the stiffness parameter λ^{-1} has been estimated to be 18 Å, which is almost the same as the values for typical flexible polymers, *e.g.*, a-PS and PIB.

For the L samples, the cloud point has also been determined in their aqueous solutions in the range of $0.5\% \lesssim w \lesssim 10\%$ by monitoring the transmittance of light through the solutions in the heating process. It has then been found that the cloud point decreases remarkably with decreasing M_w, especially in the range of $w \gtrsim 2\%$, because of the effects of the hydrophobic chain end groups of the L samples. It is more important to note that the transmittance curve for each solution does not show sharp decrease as usually observed in common LCST miscibility behavior. Such a result implies that the cloud point does not necessarily correspond to the binodal one as far as the aqueous PNIPA solutions are concerned.

Acknowledgment. This research was supported by a Grant-in-Aid for Young Scientists (B) (18750099) and in part by the global COE program "International Center for Integrated Research and Advanced Education in Materials Science," from the Ministry of Education, Culture, Sports, Science, and Technology, Japan.

Received: December 8, 2008
Accepted: January 31, 2009
Published: March 18, 2009

REFERENCES

1. T. Kawaguchi, Y. Kojima, M. Osa, and T. Yoshizaki, *Polym. J.*, **40**, 455 (2008).
2. H. G. Schild, *Prog. Polym. Sci.*, **17**, 163 (1992).
3. T. Kawaguchi, Y. Kojima, M. Osa, and T. Yoshizaki, *Polym. J.*, **40**, 528 (2008).
4. T. Kitayama, W. Shibuya, and K. Katsukawa, *Polym. J.*, **34**, 405 (2002).
5. T. Ishizone and M. Ito, *J. Polym. Sci., Part A: Polym. Chem.*, **40**, 4328 (2002).
6. M. Ito and T. Ishizone, *Des. Monomers Polym.*, **7**, 11 (2004).
7. M. Ito and T. Ishizone, *J. Polym. Sci., Part A: Polym. Chem.*, **44**, 4832 (2006).
8. O. Kratky and G. Porod, *Recl. Trav. Chim. Pays-Bas*, **68**, 1106 (1949).
9. H. Yamakawa, "Helical Wormlike Chains in Polymer Solutions," Springer, Berlin, 1997.
10. G. Deželić and J. Vavra, *Croat. Chem. Acta*, **38**, 35 (1966).
11. G. C. Berry, *J. Chem. Phys.*, **44**, 4550 (1966).
12. B. L. Johnson and J. Smith, in "Light Scattering from Polymer Solutions," M. B. Huglin, Ed., Academic Press, London, 1972, Chap. 2.
13. Y. Isobe, D. Fujioka, S. Habaue, and Y. Okamoto, *J. Am. Chem. Soc.*, **123**, 7180 (2001) and its supporting information.
14. H. Yamakawa, "Modern Theory of Polymer Solutions," Harper & Row, New York, 1971. Its electronic edition is available on-line at the URL: http://www.molsci.polym.kyoto-u.ac.jp/archives/redbook.pdf
15. H. Utiyama and M. Kurata, *Bull. Inst. Chem. Res. Kyoto Univ.*, **42**, 128 (1964).
16. H. Utiyama, *J. Phys. Chem.*, **69**, 4138 (1965).
17. K. Nagai, *Polym. J.*, **3**, 67 (1972).
18. H. Yamakawa, M. Fujii, and J. Shimada, *J. Chem. Phys.*, **71**, 1611 (1979).
19. M. Nakatsuji, Y. Ogata, M. Osa, T. Yoshizaki, and H. Yamakawa, *Macromolecules*, **34**, 8512 (2001).
20. M. Nakatsuji, M. Hyakutake, M. Osa, and T. Yoshizaki, *Polym. J.*, **40**, 566 (2008).
21. H. Yamakawa, *Macromolecules*, **25**, 1912 (1992).
22. Y. Einaga, F. Abe, and H. Yamakawa, *Macromolecules*, **26**, 6243 (1993).
23. F. Abe, Y. Einaga, and H. Yamakawa, *Macromolecules*, **27**, 3262 (1994).
24. M. Kamijo, F. Abe, Y. Einaga, and H. Yamakawa, *Macromolecules*, **28**, 4159 (1995).
25. W. Tokuhara, M. Osa, T. Yoshizaki, and H. Yamakawa, *Macromolecules*, **36**, 5311 (2003).
26. T. Mizuno, K. Terao, Y. Nakamura, and T. Norisuye, *Macromolecules*, **38**, 5311 (2005).
27. M. Osa, T. Yoshizaki, and H. Yamakawa, *Macromolecules*, **33**, 4828 (2000).
28. C. Domb and A. J. Barrett, *Polymer*, **17**, 179 (1976).
29. T. Yoshizaki, I. Nitta, and H. Yamakawa, *Macromolecules*, **21**, 165 (1988).
30. H. Yamakawa and W. H. Stockmayer, *J. Chem. Phys.*, **57**, 2843 (1972).
31. H. Yamakawa and J. Shimada, *J. Chem. Phys.*, **83**, 2607 (1985).
32. J. Shimada and H. Yamakawa, *J. Chem. Phys.*, **85**, 591 (1986).
33. A. J. Barrett, *Macromolecules*, **17**, 1566 (1984).
34. K. Kubota, S. Fujishige, and I. Ando, *Polym. J.*, **22**, 15 (1990).
35. K. Kubota, K. Hamano, N. Kuwahara, S. Fujishige, and I. Ando, *Polym. J.*, **22**, 1051 (1990).
36. J. E. Chung, M. Yokoyama, K. Suzuki, T. Aoyagi, Y. Sakurai, and T. Okano, *Colloids Surf., B*, **9**, 37 (1997).
37. J. E. Chung, M. Yokoyama, T. Aoyagi, Y. Sakurai, and T. Okano, *J. Controlled Release*, **53**, 119 (1998).
38. P. Kujawa, F. Segui, S. Shaban, C. Diab, Y. Okada, F. Tanaka, and F. M. Winnik, *Macromolecules*, **39**, 341 (2006).
39. Q. Duan, A. Narumi, Y. Miura, X. Shen, S. Sato, T. Satoh, and T. Kakuchi, *Polym. J.*, **38**, 306 (2006).
40. S. Furyk, Y. Zhang, D. Ortiz-Acosta, P. S. Cremer, and D. E. Bergbreiter, *J. Polym. Sci., Part A: Polym. Chem.*, **44**, 1492 (2006).

